ELSEVIER

Contents lists available at ScienceDirect

Journal of Molecular Liquids

journal homepage: www.elsevier.com/locate/molliq



Controlling phase separation behavior of thermo-responsive ionic liquids through the directed distribution of anionic charge



Eva M. Gulotty^a, Sidharth Sanadhya^b, Zachary D. Tucker^a, Saeed S. Moghaddam^{b,*}, Brandon L. Ashfeld^{a,*}

ARTICLE INFO

Article history: Received 20 March 2022 Revised 9 May 2022 Accepted 13 May 2022 Available online 18 May 2022

Keywords: Ionic Liquids VT NMR Separations LCST UCST COSMO-RS Sigma Profile

ABSTRACT

Thermoresponsive ionic liquids (TR-ILs) are room temperature liquid salt electrolytes with dynamic physical properties which have been hailed as potential solutions to inefficiencies in energy storage and material separations. That potential is hindered by the sensitivity of TR-IL phase separation to chemical structure. An accurate assessment of the effect of ion structure on molecular bonding is required for rational design as bonding changes translate to bulk material behavior. We systematically modify the structure of TR-ILs which exhibit either lower critical solution temperature (UCST) phase separation to isolate the effect of specific types of bonding on eight tetrabutylphosphonium benzoate derived ILs through COSMO-RS sigma profile analysis and variable temperature (VT) ¹H NMR. Our results reveal that in addition to Hydrogen bonding, cation conformational flexibility, functional group availability, cation–anion coordination strength and directionality of hydrogen bonds play key roles in governing the IL phase separation behavior.

© 2017 Elsevier Inc. All rights reserved.

© 2022 Elsevier B.V. All rights reserved.

1. Introduction

Thermo-responsive ionic liquids (TRILs) and their aqueous solutions have emerged as alternative non-volatile solvents for selective extraction processes [1–3]. The separation of a TRIL homogeneous liquid mixture into two immiscible liquids as temperature increases has the potential to mitigate the energy penalty for a broad spectrum of industrial processes including separation, drying, and distillation [2–9]. Additionally, TRILs have the potential to increase the energy efficiency of processes involving water extraction such as thermal desalination and dehumidification [10–12].

Despite recent studies aimed at developing a predictive measure for LCST phase separation behavior, a fundamental understanding of the underlying molecular interactions remains elusive, and is critical for accurate structure–function relationships. Pioneering work by Ohno and coworkers has implicated the relative hydrophilicity of anions and cations in thermoresponsive ionic liquids (TRILs) as primary considerations in LCST behavior (Fig. 1a) [13–17]. However, hydrophilicity and the relative contributions from H-bond donors and acceptors derive from a

 $\hbox{\it E-mail addresses: } saeedmog@ufl.edu (S.S. Moghaddam), bashfeld@nd.edu (B.L. Ashfeld).}$

diverse array of structural attributes that include conformational flexibility, charge distribution, acidity, and molecular symmetry. Similarly, water hydration shells are typically characterized by a higher degree of organization and a greater number of strong H-bonds than are typically found in bulk water bonding.[18–19] As temperature is increased, the ordered structure of the hydration shell gives way to a more disordered framework comprised of weaker H-bonding as entropy begins to dominate. This disruption of water hydration shell structure leads to increased aggregation as the phase transition temperature is approached. (Fig. 1b).[20] The temperature-controlled strength and conformational flexibility of water-water, IL-IL, and water-IL bonds affect the balance between entropy and enthalpy in LCST phase separation.

To better understand the underlying chemical physics of LCST behavior in ILs, we evaluated a designed subset of fluids to specifically probe those architectural features critical to this underutilized and peculiar phenomenon. We speculated that the strength and location of cation coordination, the localization of charge density across the anion, and the directionality of interand intramolecular H-bonding play a dominant role in both LCST behavior and the magnitude of phase separation temperature (Fig. 1c). Specifically, we examined a series of previously known and unknown TRILs in aqueous solutions to identify key temperature-dependent bonding changes that contribute to LCST phase separation. In contrast to previous reports relating LCST

^a Department of Chemistry and Biochemistry, University of Notre Dame, Notre Dame, IN 46556, USA

^b Department of Mechanical and Aerospace Engineering, University of Florida, Gainesville, FL 32608, USA

^{*} Corresponding authors.

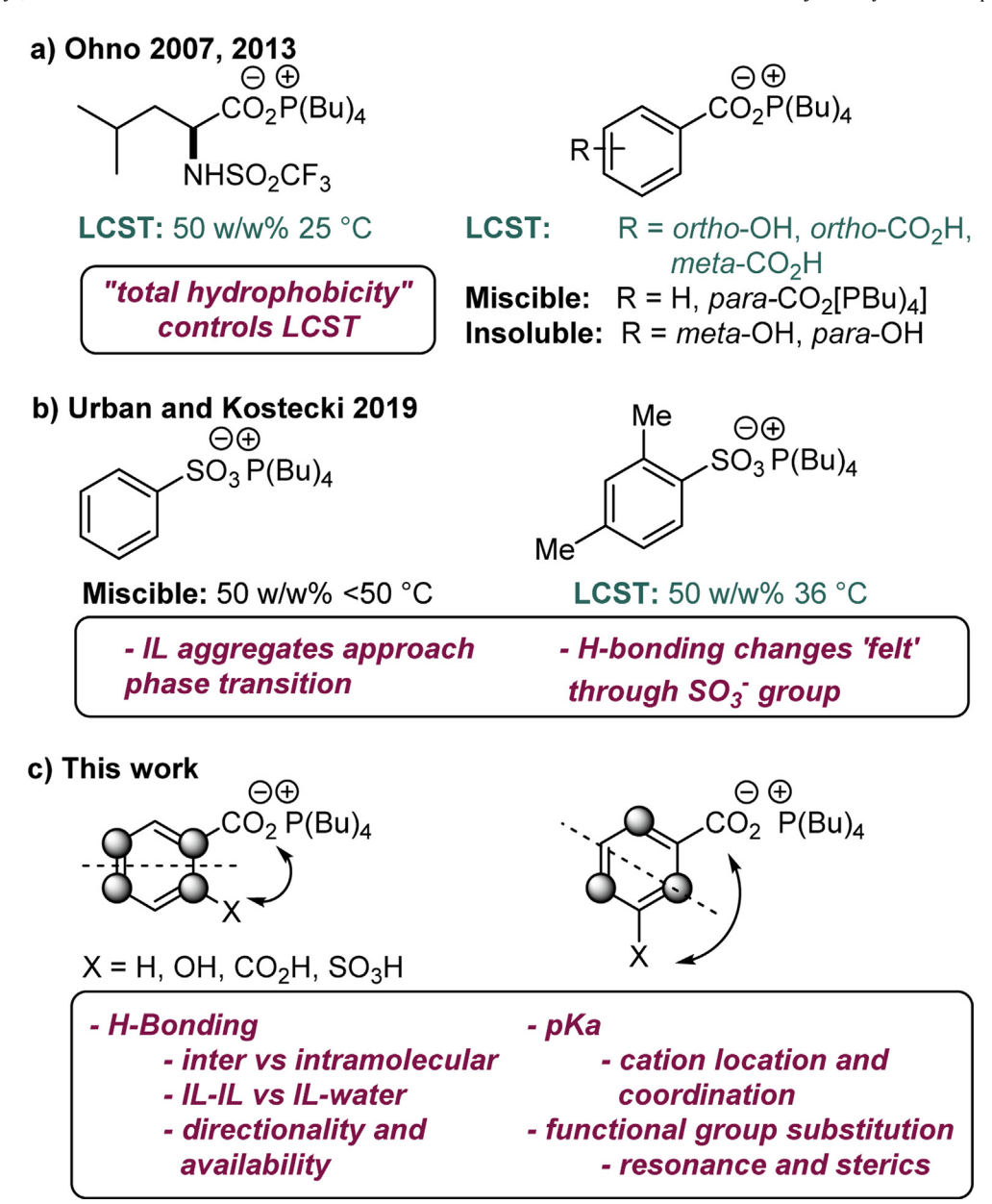


Fig. 1. a) Hydrophobic LCST TRILs established by Ohno et. al., b) Urban and Kostecki determined aggregation and H-bonding changes leading to LCST phase separation, c) this work: a systematic structure-behavior study to determine the effect of anion structure on bonding changes which drive LCST TRIL behavior.

behavior to the strength of H-bonding, our composite findings revealed a strong dependency on the accessibility and charge density of the anion as a dominant factor in the manifestation of LCST phase separation.

Given the notable role of H-bonding in phase separation, we began by examining the strength and directionality of H-bond donor/acceptor functionality on IL anions and their contributions to LCST phase separation.[21–23] To isolate these contributing factors, we focused on a series of conformationally constrained benzoate-derived IL anions paired with the tetrabutylphosphonium cation, with systematic structural modifications to the benzoate anion (Fig. 1).[16] For those ILs with *ortho*-substituted aryl rings, phase separation behavior is often difficult to predict due to a delicate balance of factors which include intra- and intermolecular H-bonding, steric interactions, and functional group proximity.[24] For example, while an aqueous solution of 1 (80 wt% in water) exhibits UCST separation with a phase transition temperature of 46 °C, the presence of an *ortho*-hydroxyl group in

benzoate $\mathbf{2}$ (67 wt% in water) undergoes LCST phase separation at 62 °C.[15].

2. Results and discussion

2.1. Benzoate (1) vs. ortho-hydroxybenzoate (2)

To investigate the impact of H-bonding in **2**, we examined the COSMO-RS σ -profiles of ILs **1** and **2** by calculating the surface charge distribution of the IL and its theoretical dipole moment in water. The σ -profile is based on the solvent accessible surface, and exhibits a peak at a negative σ if an area of the molecule is an H-bond donor, a peak at a positive σ if an area is an H-bond acceptor, and a peak between -0.08-0.08 e/A² if the molecule is exhibiting non-traditional H-bonding (e.g., bonding with the π -cloud of the aryl ring, Van Der Waals interactions, etc.).[25–27] The relative intensity of the σ -profile peaks correlates to the magnitude of the bonding potential for that ion. The σ -profile for **1**

depicts the carboxylate as a peak at 0.018 e/A² indicating H-bond accepting properties (Fig. 2a). Likewise, the carboxylate anion in 2 is represented by a relatively broad H-bond acceptor peak at 0.016 e/A² indicating a more dynamically flexible intra-/intermolecular H-bonding motif. This broadening is consistent with a temperature-dependent, intramolecular H-bond between the 1-OH hydrogen and carboxylate groups in competition with H-Bonding to the water solvation shell (Fig. 2a). The phenyl ring also participates as a non-traditional H-bond acceptor through the π -electron cloud, as represented by peaks at 0.005 e/A² for both 1 and 2.

To gain insight into the temperature-dependent inter/intramolecular interactions within the molecular environment of each IL during phase transition, we used variable temperature (VT) ^1H NMR to assess the chemical shift differences in an aqueous solution. Though we anticipated the *para*-Hg would display the greatest temperature dependent peak shift due to a change in cation–anion coordination strength and bond length, IL 1 exhibited a linear peak shift (Δppm) for hydrogen 1-Hg with a Slope of 4.05 x10-04 ppm/°C, while 2-Hg showed no significant slope (see supporting information). Though the peak shift slopes for hydrogens 1-Hg and 2-Hg were similar in magnitude, the *meta*-hydrogens 1-

H^f revealed a threefold increase relative to **2**-H^f in temperature dependence (Fig. 2b). Without the resonance stabilization from the hydroxyl group that **2**-H^f experiences, only the σ-withdrawing inductive effect of the carboxylate affects **1**-H^f, which leads to localized electron deficiency at the *meta*- position. The π -donation of the *ortho*- **2**-OH group counteracts this *meta*-inductive effect of the carboxylate by increasing electron density at the **2**-H^f and **2**-H^h positions, which is also the cause of a greater electron cloud dispersion across the anion of **2** resulting in a broader σ-profile.

Changes in the magnitude and directionality of H-bonding between the IL and the water solvation shell correlated to changes between IL 1 and 2 phase separation behavior. The water resonances in an aqueous solution of IL 1 displayed a cluster of three major peaks $(1-H_2O^a, 1-H_2O^b, \text{ and } 1-H_2O^c)$, which were shifted to a more electron rich environment by -0.38 ppm (Fig. 2c). In contrast, the water region of 2 exhibited two distinct resonances correlating to the bulk water environment, $(2-H_2O^a)$ and IL-solvated water $(2-H_2O^b)$. The UCST-exhibiting aqueous solution of 1 shifted the water resonances to a more electron rich environment by an average of 0.5 ppm relative to the LCST IL 2 water shifts due to the additional electron density withdrawn by the 2-OH from the

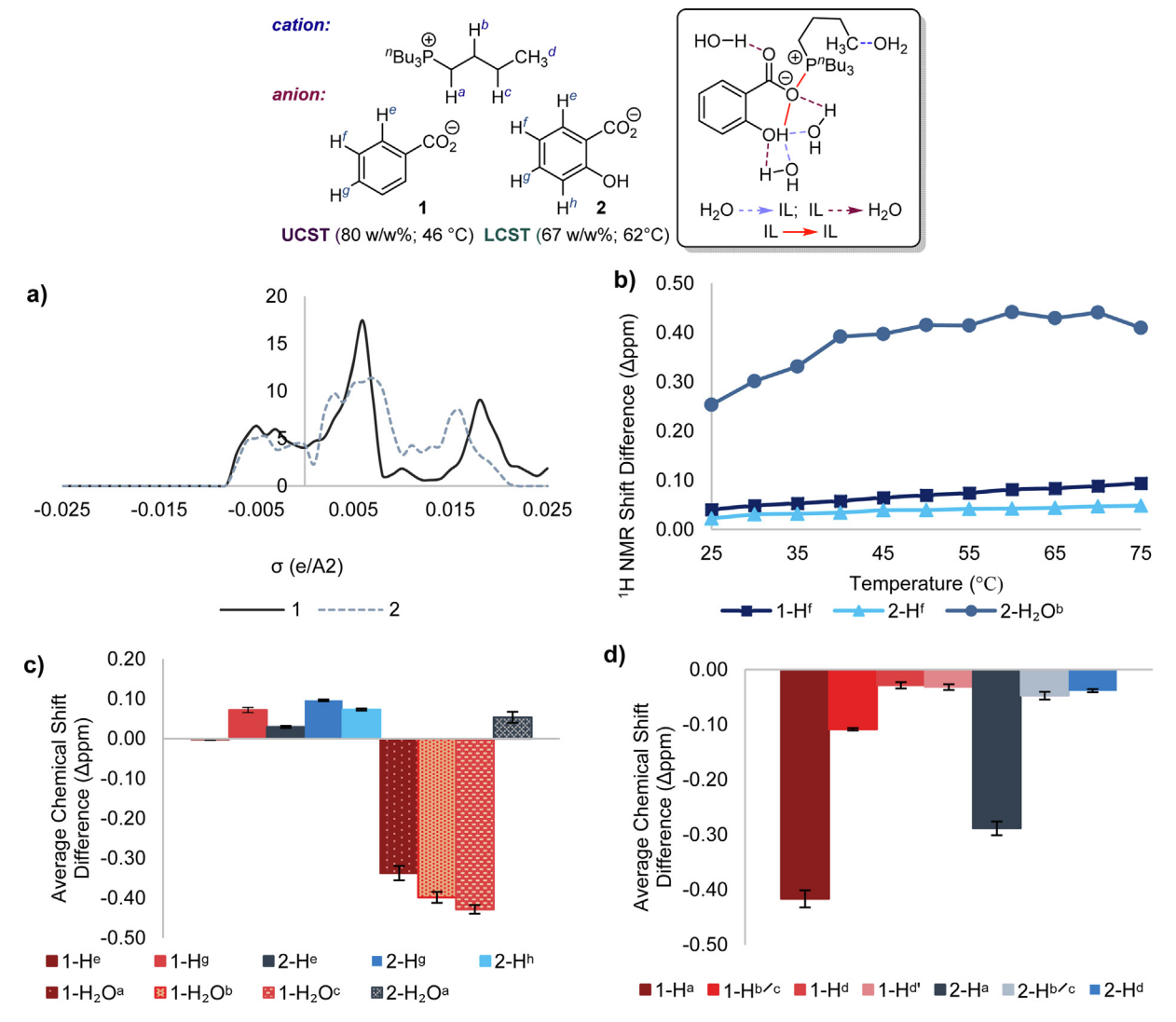


Fig. 2. Phase separation behavior and key bonding interactions for ILs 1 and 2: a) COSMO-RS σ -profiles, (See Supplementary Table 1); b) Temperature dependent ¹H NMR shift differences (Δ ppm) in aqueous solutions from 25 to 75 °C; c) Average anion and water resonance Δ ppm in aqueous solutions, d) Average cation Δ ppm in aqueous solutions from 25 to 75 °C.

water solvation shell (Fig. 2b and 2c). The shift to lower frequency of **2**-H₂O^b by 0.25–0.4 ppm indicates an H-bond directionality in the IL-rich environment wherein electron density is transferred from the bulk water to the IL through the 2-OH group. The magnitude of the change in ¹H NMR shift for cation resonances H^{a-d} for **1** and 2 exponentially decayed as the hydrogen location moved away from the charged phosphorus for both ILs (Fig. 2d). Although the cation resonances rarely changed with temperature, 1-Ha exhibited a linear dependence of 9.79 x10⁻⁰⁴ ppm/°C due to varying cation– anion and water shell coordination strength as temperatures increased and the alkyl chain entropy dominated. Additionally, ¹H NMR peaks for both the cation resonances associated with 1-Ha and the anion resonance 1-He exhibited a sudden increase in Δppm averaging 0.004 ppm at 60 °C, which was mirrored by a sudden decrease in Δ ppm for water peaks **1**-H₂O^a, **1**-H₂O^b, and **1**-H₂O^c, also averaging -0.04 ppm as direct evidence of a sudden change in IL-water bonding where water regains a higher bonding order while the anion and cation lose that electron density (Table 1). No such Δppm deviation was observed for **2**, as both IL and water shift changes were gradual.

2.2. H-bond directionality and strength: ortho-carboxybenzoate (3)

The differences in bonding between **1** and **2** reflect a more complicated system than is represented by the magnitude of H-bonding or overall hydrophobicity, with nonlinear H-bonding and cation–anion bonding changes in UCST IL **1**, and a switch in the directionality of H-bonding for LCST IL **2**. Similar to **2**, the benzoate-derived IL **3** bears a strong H-bond donor –CO₂H, and displays LCST phase separation in aqueous solution at 50 wt% and 60 °C (Fig. 3).[15] While the σ -profile of **3** is similar to the unsubstituted benzoate IL **1**, the carboxylate bonding peak is more intense, broader, and is shifted to 0.014 e/A² indicating that charge distribution across the anion is less accessible for H-bonding (Fig. 3a). The σ -profile shift of –0.004 e/A² is most likely due to the stronger, intramolecular H-bonding between the **3**-carboxylate anion and **3**-CO₂H.

The VT ¹H NMR analysis of **3** in an aqueous 50 w/w% solution revealed that **3**-H^f experienced a slight linear temperature-dependent shift with a 7.46x10⁻⁰⁴ ppm/°C slope (Fig. 3b). The **3**-CO₂H has two additive factors that increase the **3**-H^g slope relative to **1**-H^g and **2**-H^g. First, the cation of **3** exhibits conformational flexibility while coordinating closely with one or both carboxy groups, which allows water to interrupt the ion pair bonding and diminish the inductive effect at the *para*- position. Second, the temperature dependent variations in water H-bonding to the protonated carboxylic acid directly affect its inductive strength and electron donation strength as temperatures change.

Overall, electron density was lost by the water shell and the shift to lower frequency of ${\bf 3}\text{-H}_2O^b$ by 0.56 ppm reflects the disruption of water-water H-bonding by the carboxylic acid functionality (Fig. 3b). Like UCST 1, LSCT IL 3 exhibited a notable Δ ppm change at 55–60 °C. Below this temperature, the cation methyl group peaks (${\bf 3}\text{-H}^d$) were deshielded by 0.008 ppm, which was followed by the three distinct water resonances ${\bf 3}\text{-H}_2O^a$, ${\bf 3}\text{-H}_2O^a$, and ${\bf 3}\text{-H}_2O^c$ exhibiting a shift to lower frequency of -0.042 ppm 60 °C (Table 2).

Table 1 1 H NMR Δ ppm of aqueous UCST IL 1 at 60 $^{\circ}$ C.

Anion ¹ H	∆ppm	Water ¹ H	∆ppm
H ^e H ^a	0.0024 0.0036	H_2O^a H_2O^b	-0.0448 -0.0403
H ^{a'}	0.0048	H_2O^c	-0.0389

2.3. Directing cation location with pKa: ortho-sulfonylbenzoate (4)

The sulfonate-based IL **4**, wherein the sulfonate anion resides ortho- to the benzoic acid functionality, displayed UCST behavior at 60 °C in 50 w/w% with water, and provided a direct functional group comparison to the carboxylate- and phenol-bearing LCST ILS 2 and 3. Incorporation of the less basic -SO₃ anion results in a stronger ionic interaction with the cation than what is typically observed with carboxylates or phenoxide moieties.[15,28] This anion-cation interaction, with a bulky phosphonium cation, can reduce the extent of H-bonding with the sulfonate and provides another dynamic bonding parameter to consider for TR separation behavior. The σ -profile for **4** displays an intense H-bond acceptor peak at 0.016 e/A² which is twice the magnitude of that observed for **2** (Fig. 3a). The π -bonding peak for **4** is less intense than for **1** and **3** and has a reduced value of 0.003 e/A², which is consistent with the greater electron withdrawing properties of the sulfonate group. An electron acceptor peak was also observed from -0.02 to -0.01 e/A^2 on the σ -profile of **4**, correlating to H-bond donation from the available CO₂H.[27,29] Likewise, the electron withdrawing sulfonate leads to a significant 0.38 ppm deshielding of the **4**-H^e hydrogen relative to **3**-H^e (Fig. 3c). Conversely, the carboxylic acid proton in 4 was shifted to lower frequency by -0.6 to -0.5 ppm due to significant H-bonding with the water solvation shell, leading to disruption of water-water bonding which also shifts the 4-H₂O^a peak to a higher frequency by 0.75-1.0 ppm (Fig. 3b). The cation of 4 exhibited the least chemical shift change, with a Δ ppm of -0.14 ppm for **4**-H^a in water. This small solvation effect is due to the strength of the sulfonate-phosphonium ion pair, leading to reduced water intrusion. These results indicate that the phase separation for UCST IL 4 is driven not simply by cation-water hydrophobic and entropic parameters, but rather anion-water interactions and the balance of electron density between the withdrawing sulfonate and donation of water to the CO₂H.

2.4. Acid effect on H-bonding: ortho-sulfonatobenzoate (5)

To probe the impact of H-bond directionality on phase separation behavior, we then examined the contribution of CO₂H and SO₃H H-bond donor groups. The presence of a CO₂H group is reported to affect the temperature sensitivity of the hydration shell structural organization.[30–31] By removing the hydrogen entirely in the di-anionic sulfonyl benzoate IL 5, the CO₂H hydrogen was removed and the conformational flexibility of the cation was constrained (Fig. 3). Despite the absence of intramolecular H-bonding, IL **5** exhibited comparable UCST separation behavior to **4** at 60 °C. Though both ILs exhibit UCST phase separation behavior, the water peak 5-H₂O^a was shielded by -1.0 ppm relative to 4-H₂O^a indicating a reversal of bond directionality with the water shell (Fig. 3b, 3c). This water solvation energy drives the temperaturedependent bonding and is the controlling factor in UCST phase separation for 5. A net increase in water H-bonding was observed via the **5**-H₂O^a shift to higher frequency by -0.2 ppm while **5**-H₂O^b was shifted -0.8 ppm with strong linear temperature dependence and a slope of 1.04x10⁻⁰² ppm/°C as the dianion of **5** increasingly donated electron density to the IL solvated water with increasing temperatures (Fig. 3b, 3c). The cation 5-Ha is also shielded -0.45 ppm by electron density from the water shell while 5-He was deshielded 0.30 ppm, which implicates an overall increase of both bonding to the water solvation shell and water-water bonding as the source of electron density.

2.5. Proximity and availability: meta-substituted ILs (6-8)

The dominant bonding motifs between each of the *ortho*-substituted benzoate ILs **2–5** and water varied depending on the

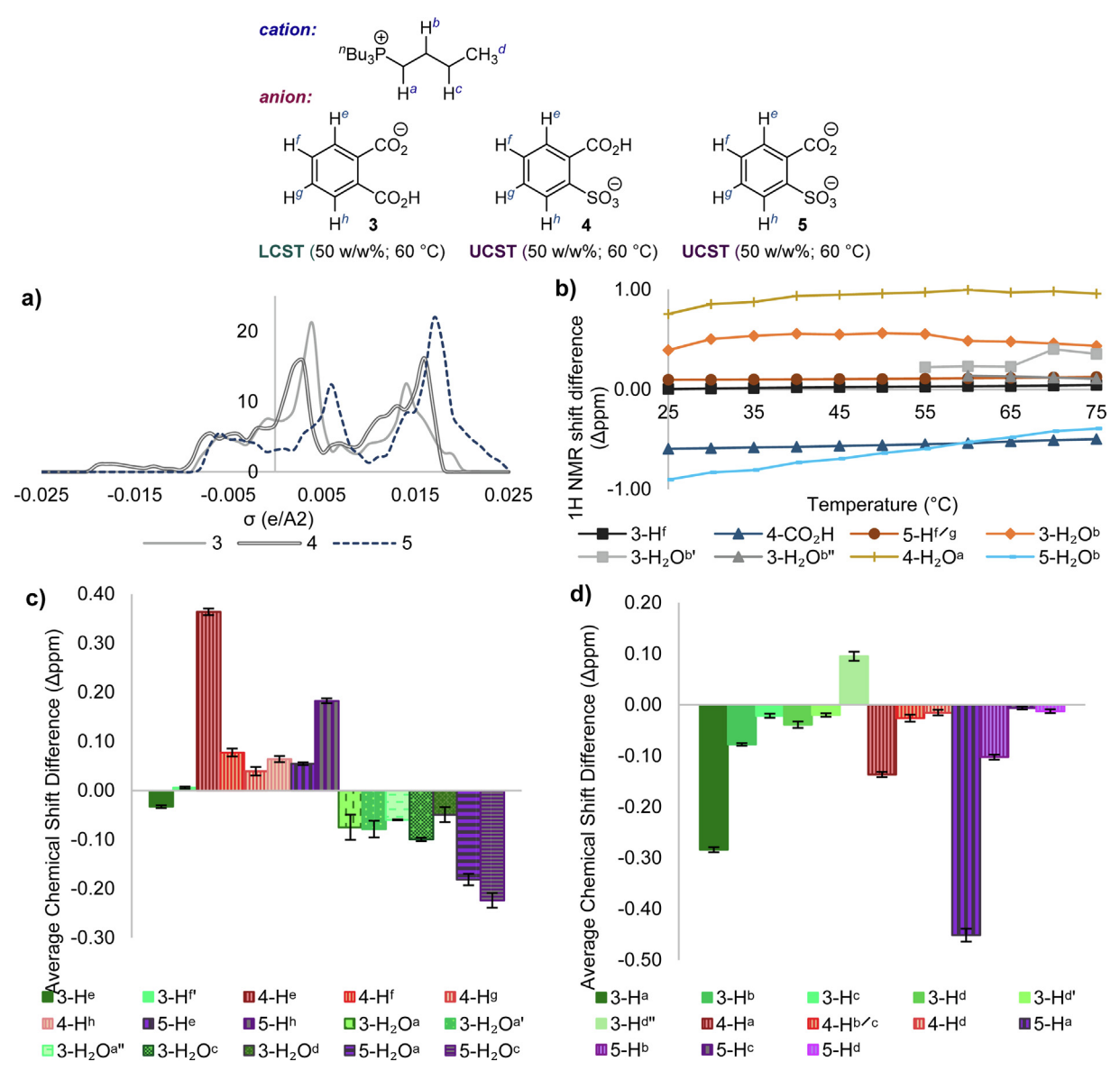


Fig. 3. Phase separation behavior for ILs 3–5: a) COSMO-RS σ-profiles, (See Supplementary Table 1); b) Temperature dependent ¹H NMR shift differences (Δppm) in aqueous solutions from 25 to 75 °C; c) Average anion and water resonance Δppm in aqueous solutions from 25 to 75 °C, d) Average cation Δppm in aqueous solutions from 25 to 75 °C.

Table 2 1 H NMR Δ ppm of aqueous LCST IL **3** at 55–60 $^{\circ}$ C.

Anion ¹ H	Δ ppm	Water ¹ H	∆ppm
H ^a	0.0096	H ₂ O ^a	-0.0488
H ^{a'}	0.0088	H ₂ O ^{a'}	-0.0348
H ^{a''}	0.0057	H ₂ O ^d	-0.0437

functional groups involved. Postulating that the directionality of H-bonding for the more accessible $\it meta$ -substituted ILs would significantly alter the nature of IL-water bonding, we next studied the analogous $\it meta$ - substituted ILs **6–8** (Fig. 4). Benzoate ILs **6–8** have a substitution pattern which prevents the anion from participating in intramolecular H-bonding. IL **6** exhibits LCST behavior with an intermolecular H-bond donor peak in the σ -profile between - 0.01 and -0.02 e/A 2 (Fig. 4a). Notably, IL **6** is insoluble in water at room temperature, but undergoes LCST separation at 35 $^{\circ}$ C in an aqueous 30 w/w% solution. The VT 1 H NMR spectra of **6** revealed three distinct anion bonding environments, characterized by three chemically distinct signals for the anion hydrogens wherein the $\it m$ -

hydroxy group experiences an increase in shielding from water H-bonding leading to an increase in chemical shift frequency for the ${\bf 6}\text{-H}^{\rm h}$ hydrogen environments (Fig. 4b, 4c). While ILs ${\bf 2}$ and ${\bf 6}$ exhibit LCST separation, the promotion of stronger temperature-dependent intermolecular H-bonding by the –OH group in ${\bf 6}$ presumably leads to a higher melting point.

The *meta*-CO₂H substituted sulfonate IL **7** also displays a higher melting point than its *ortho*-substituted analogue (Fig. 4). Interestingly, while 1,2-carboxy sulfonate IL **4** undergoes UCST phase separation at 60 °C in 50 w/w% with water, the 1,3-carboxy sulfonate IL **7** exhibits LCST phase separation at the same temperature and concentration. This result would indicate that the relative orientation of H-bonding donor/acceptor influences IL-water phase separation behavior. In contrast to the strong and weak binding modes observed in IL **4**, its constitutional isomer **7** exhibits two equally strong peaks at 0.012 e/A² and 0.014 e/A² in the σ -profile, presumably the result of the availability of both sulfonate and carboxylate groups for H-bonding (Fig. 4a). Additionally, the non-traditional H-bonding peak for **7** is less intense than that of **4** as bonding localizes on the attached functional groups. While ILs **4** and **7** each con-

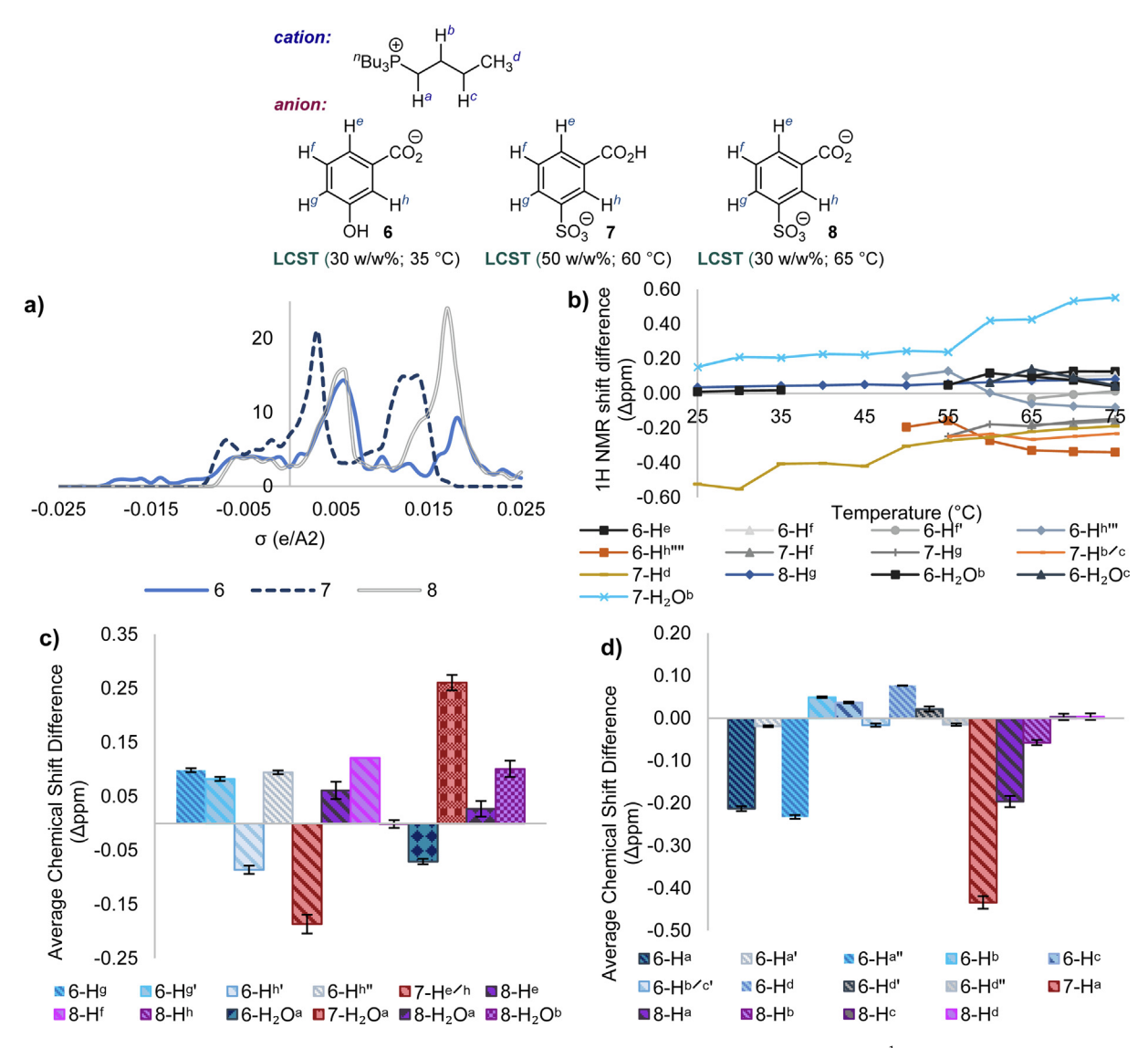


Fig. 4. Phase separation behavior for ILs 6-8: a) COSMO-RS σ -profiles, (See Supplementary Table 1); b) Temperature dependent 1 H NMR shift differences (Δ ppm) in aqueous solutions from 25 to 75 °C; c) Average anion Δ ppm in aqueous solutions and water resonances, d) Average cation Δ ppm in aqueous solutions from 25 to 75 °C.

tain a carboxylic acid group, **7**-H^e is deshielded by 0.56 ppm due to the 1,4-relationship of the sulfonate, and the remaining anion peaks are shifted to a lower frequency by -0.30 ppm due to the increased accessibility of 7-CO₂H for H-bonding to the water shell (Fig. 4c). Surprisingly, no H-bond donation peak between -0.01 and -0.02 e/A² was observed for **7** (Fig. 4a). Additionally, we observed notable increase in the electron density in the ¹H NMR for aqueous 7 above 55 °C relative to neat IL, with the greatest effect observed for the cation alkyl chains (Fig. 4c, 4d). This electronic change for both cation and anion differ from the impact of water solvation observed for IL 5, in that 7-H₂O^a and 7-H₂O^b peaks both lose electron density when drawn into IL-water bonding (Fig. 4c). The bulk water in an aqueous solution 7-H₂O^a experiences less H-bonding density than pure water, with a shift to higher frequency via ¹H NMR of 0.25 ppm, which is less than the 0.95 ppm higher frequency shift for **4**-H₂O^a for which H-bonding is more disrupted.

In contrast, the LCST dianionic *meta*-sulfobenzoate IL **8**, which lacks an H-bond donor group, exhibited comparable phase transition behavior to **7** in 30 w/w% water at 65 °C but is a liquid at room temperature and more soluble in water than **7** (Fig. 4). The σ -profile for **8** closely resembles the *ortho*-dianion **5** with a strong H-bond acceptor peak at 0.017 e/A² and a π -donor peak at 0.007

e/A² (Fig. 4a). In comparison to **7**, the effect of **8** on water via 1H NMR is minor, with a five-fold decrease in Δppm (Fig. 4c, 4d). Though the magnitude of bonding change for water between **8** solution and water self bonding was small, both the anion **8**-H² and cation **8**-H² peaks displayed a change in Δppm like **1** and **3**, with **8**-H² and **8**-H² deshielded an average of 0.032 ppm and **8**-H³ shielded by -0.035 ppm. In contrast to ILs **1** and **3**, the water peaks in an aqueous solution of **8** did not exhibit any sudden change in Δppm (Table 3). Only **4** had a smaller H³ Δppm magnitude than **8**, with **8**-H³ only shifting -0.2 ppm with water solvation. Since we attributed this low Δppm in **4** to a strong anion-cation interaction, we speculated that the similar Δppm in **8** was due to either

Table 3 1 H NMR Δ ppm of aqueous LCST IL **8** at 50 $^{\circ}$ C.

Anion ¹ H	∆ppm
He	0.0341
H^f	0.0284
H ^a	-0.0350

the electron rich anion mimicking water bonding or a strong anion pairing to the phosphonium cations.

2.6. Ion pair strength via ¹H DOSY NMR

We were able to observe the cation-anion bond strength spectroscopically via the temperature-dependent magnitude of H^a and diffusion coefficients (D) determined through VT ¹H Diffusion Ordered Spectroscopy (DOSY) NMR. Diffusion constants correlate to mass transport throughout the IL while providing a handle for comparison of ion pair strength and relative anion and cation interactions with water. Differences in D also indicate the relative contribution of each ion to the mass transport of the system.[32–34] Dications such as 5 and 8 have been shown to significantly effect diffusion and the energy required for water solvation.[35] Comparison of the VT ¹H DOSY NMR shift differences show a loosening of the ion pair as temperatures increase for 2 and 5, and a lower magnitude of D difference for 1 and 4. whereas 8 exhibited almost no difference in D between cation and anion (Fig. 5). The cause of the weakened ion pair displayed by 2 is the temperaturedependent intramolecular H-bonding which dominates at lower temperatures. As temperatures increase, water solvates the phosphonium cation of 5, leading to the large 5-H^a Δppm (Fig. 3e). The cation coordination for 1 and 4 is more localized, and thus a less dynamic bonding change is observed. IL 8 showed the least difference between cation and anion diffusion constant, indicating this IL is solvated as an intact trio of ions with weaker bonds to other IL ion groups in solution.

Positively charged species with coupled hydrophobic and hydrophilic behavior have been shown to perturb a hydrophobicwater interface differently than negatively charged ambiphilic species, with anionic surfactants stabilizing the interfacial water through organization of the water dipoles as they align with the negatively charged head.[36-37] In contrast, positively charged hydrophobic/hydrophilic species do not induce water organization, rather the interfacial hydrophobic phase conformational flexibility is altered and water directionality is decreased.[36-37] The directionality of H-bonding reverses for the carboxylic acid groups of 4 and 7 versus the carboxylate functional groups of 5 and 8 where the sulfonate preferentially coordinates the tetrabutylphosphonium cation, leaving the carboxylic acid groups accessible for Hbonding. These interactions indicate the steric availability of the sulfonate functional group as well as the strength of H-bonding and the symmetry of the aryl orbitals derived from the substitution pattern all contribute to the complexity of IL-water bonding, and the differing phase separation behavior of ILs 1-8.

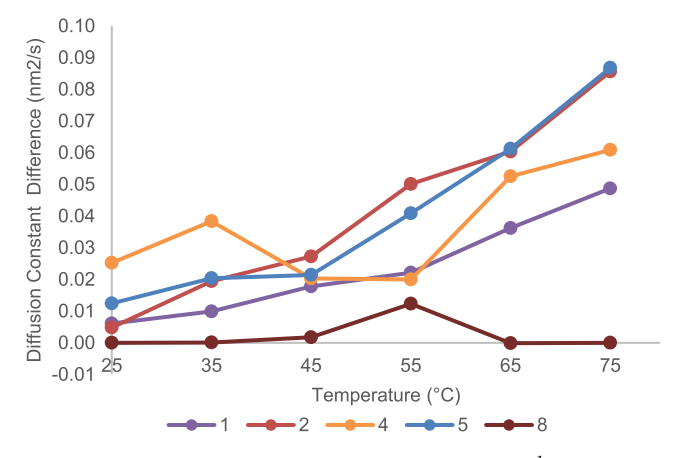


Fig. 5. Changes in the diffusion constant (D) from 25 to 75 °C via ¹H DOSY NMR for ILs **1**, **2**, **4**, **5**, and **8**.

3. Conclusion

In conclusion, the effects of H-bond strength and directionality. cation-anion coordination strength and localization, and functional group accessibility on phase separations for IL-water systems were investigated using predictive models and VT NMR spectroscopy. A detailed comparison of the functional group Hbond strength trends revealed that intramolecular H-bond donation strength is not solely responsible for the control of LCST phase separation. We determined the contribution of H-bond donor groups to LCST phase separation by comparing di-anionic sulfobenzoates and found that although the phase separation behavior is not affected by H-bond directionality, it had a strong effect on IL-water solvation. Preferential coordination controlled by functional group pKa can disrupt and direct H-bonding, directly affecting the bonding equilibrium that manifests as LCST separation. These features derive from the IL anion substitution pattern and provide a more complex understanding of the structural contributions to the parameters which direct LCST phase separation in aqueous solutions.

4. Experimental methods

4.1. Experimental procedure for VT NMR Collection:

For neat IL samples, IL was weighed into a WGS-5BL Wilmad-LabGlass coaxial insert, agitated and heated as needed with a heat gun until fully settled and bubbles were not observed.[38] Then trimethoxybenzene and deuterated toluene were charged in a 5 mm 7" NMR precision sample tube. The coaxial insert was inserted in the precision sample tube, and the tubes were capped and wrapped with Teflon tape. The sample was inserted into a 500 MHz Bruker NMR at room temperature, then equilibrated to 25 °C. The temperature was raised in 5 °C increments and equilibrated for at least 10 min before ¹H and ³¹P NMR spectra were collected; Additionally, ¹H DOSY NMR data was collected in 10 °C increments.[32-33,39] Data processing was performed with a combination of Bruker Topspin, Bruker Dynamics Center, and Excel. The error in D Io measurement as estimated by Topspin was < 1%. We did not repeat all measurements, however replicating one DOSY measurement led to a deviation of < 5% in D for IL 1. Aqueous solutions of IL were weighed into a secondary vial with a screw top cap and stirred at least 6 h at room temperature. The aqueous samples were then transferred to a WGS-5BL Wilmad-LabGlass Coaxial Insert, and the sample was otherwise prepared as described above. When separate layers were observed at room temperature, the tube was aligned such that the spectrometer focus was 2 mm below the interface before beginning data collection.

4.2. General experimental

Solvents and reagents were reagent grade and used without purification unless otherwise noted. Tetrahydrofuran (THF), acetonitrile (MeCN), dichloromethane (DCM), toluene (PhMe), diethyl ether (Et₂O), and dimethyl formamide (DMF) were passed through a column of molecular sieves and stored under argon. Molecular sieves were activated by heating under vacuum 30 min, left to come to room temperature under vacuum overnight, and stored in an oven at least three days before use. Unless otherwise specified, reagents were obtained from commercial sources and used without further purification. All reactions were carried out in oven dried glassware under nitrogen unless otherwise specified. ¹H nuclear magnetic resonance (NMR) spectra were obtained at 500 or 400 MHz. ¹³C NMR were obtained at 126 or101 MHz. ³¹P NMR

were obtained at 162 or 202 MHz as indicated. Chemical shifts are reported in parts per million (ppm, δ), and referenced from internal TMS standard or from solvent residual signals. Coupling constants are reported in Hertz (Hz). Spectral splitting patterns are designated as s, singlet; d, doublet; t, triplet; q, quartet; m, multiplet; comp, complex; app, apparent; and br, broad. Infrared (IR) spectra were obtained using a Thermo Electron Nicolet 380 FT-IR using a silicon (Si) crystal in an attenuated total reflectance (ATR) tower and reported as wavenumbers (cm-1). High- and low-resolution electrospray ionization (ESI) measurements were made with a micro time of flight mass spectrometer (microTOF-MS) or a microTOF-Q III liquid chromatography mass spectrometer. Analytical thin layer chromatography (TLC) was performed using EMD 250 µm 60 F254 silica gel plates, visualized with UV light and stained with either p-anisaldehyde, ninhydrin or potassium permanganate solutions. Flash column chromatography was performed according to Still's procedure using Silicycle SiliaFlash P60 40-63 µm 60 Å silica gel.[40].

4.3. Experimental procedures

4.3.1. Tetrabutylphosphonium benzoate (1).[15]

To a 100 mL round bottom flask equipped with a magnetic stir bar was added ⁿBu₄PBr (2.00 g, 5.89 mmol), placed under an atmosphere of N₂, and diluted with MeOH (6 mL). To this solution was added 2 M KOH in MeOH (6.40 mmol, 3.2 mL). Precipitation was observed upon stirring at rt for 12 h, and the resulting suspension was filtered and rinsed with MeOH (3 \times 10 mL). To the filtrate was added benzoic acid (0.704 g, 6.27 mmol) and stirred at rt for 12 h. The resulting solution was concentrated under reduced pressure, reconstituted in acetone (10 mL), and filtered through Celite. The filter cake was washed with acetone (3 \times 10 mL) and the filtrate concentrated under reduced pressure. The residue was then dried in a vacuum oven at ~ 80 °C for 48 h to provide 1.83 g (82% yield) of 1 as a clear oil that upon cooling solidified to a colorless wax. Spectral data were consistent with literature values: ¹H NMR (400 MHz, CDCl₃) δ 8.11–8.05 (comp, I = 3.3 Hz, 2H), 7.33–7.22 (comp, I = 3.1 Hz, 3 H), 2.42 (m, I = 5.1 Hz, 8 H), 1.50 (app t, I)I = 3.7 Hz, 16H), 0.95 (t, I = 6.8 Hz, 12H); ³¹P NMR (162 MHz, CDCl₃) δ 32.9 (${}^{1}J_{PC}$ = 21.7 Hz, ${}^{2}J_{PC}$ = 6.9 Hz); ${}^{13}C$ NMR (101 MHz, CDCl₃) δ 171.6, 140.8, 129.4, 128.5, 127.1, 24.0 (J_{PC} = 21.6 Hz), 23.9, 18.9 $(I_{PC} = 47.5 \text{ Hz})$, 13.5; HRMS (ESI) m/z: measured 259.252608 $C_{16}H_{36}P^{+}$ (M) requires 259.254914, HRMS (ESI) m/z: measured 121.023260 C₇H₅O₂ (M) requires 121.029503.

4.3.2. Tetrabutylphosphonium 2-hydroxybenzoate (2).[15]

To a 100 mL round bottom flask equipped with a magnetic stir bar was added ⁿBu₄PBr (7.37 g, 21.72 mmol), placed under an atmosphere of N₂, and diluted with MeOH (6 mL). To this solution was added 2 M KOH in MeOH (6.40 mmol, 3.2 mL). Precipitation was observed upon stirring at rt for 12 h, and the resulting suspension was filtered and rinsed with MeOH (3 \times 10 mL). To the filtrate was added 2-hydroxybenzoic acid (3.00 g, 21.72 mmol) and stirred at rt for 12 h. The resulting solution was concentrated under reduced pressure, reconstituted in acetone (10 mL), and filtered through Celite. The filter cake was washed with acetone $(3 \times 10 \text{ mL})$ and the filtrate concentrated under reduced pressure. The residue was then dried in a vacuum oven at \sim 80 °C for 48 h to provide 7.15 g (83%) of 2 as a clear oil that over time solidified to a tan wax. Spectral data were consistent with literature values: ¹H NMR (400 MHz, CDCl₃) δ 7.91 (dd, J = 7.6, 1.9 Hz, 1H), 7.20 (td, I = 7.6, 1.9 Hz, 1H), 6.77 (d, I = 8.1 Hz, 1H), 6.69 (t, I = 7.6 Hz, 1H), 2.13 (ddt, I = 13.1, 8.1, 5.1 Hz, 8H), 1.43 (dq, I = 9.4, 5.7, 4.5 Hz, 16H), 0.91 (t, J = 6.8 Hz, 12H); ¹³C NMR (100 MHz, CDCl₃) δ 173.0, 162.5, 131.9, 130.5, 119.9, 116.7, 116.1, 23.7 (d, J = 15.2 Hz), 23.4 (d, J = 4.8 Hz), 18.3 (d, J = 47.4 Hz), 13.3; ³¹P NMR (162 MHz, CDCl₃) δ 32.7; HRMS (ESI) m/z: measured 259.255297 C₁₆H₃₆P⁺ (M) requires 259.254914, HRMS (ESI) m/z: measured 137.022014 C₇H₅O₃ (M) requires 137.024418.

4.3.3. Tetrabutylphosphonium 2-carboxybenzoate (3).[15]

A solution of "Bu₄PBr (2.00 g, 5.89 mmol) and potassium hydrogen phthalate (1.22 g, 5.95 mmol) in acetone (6 mL) was stirred at rt for 3 d then concentrated under reduced pressure and filtered to remove potassium salts. The residue was then dried in a vacuum oven at ~ 80 °C for 48 h to provide 2.18 g (87%) of **3** as a clear oil that upon cooling solidified to a colorless wax. Spectral data were consistent with literature values: ¹H NMR (400 MHz, CDCl₃) δ 8.38 (app dq, J = 5.9, 3.4 Hz, 2H), 7.48 (app dq, J = 5.9, 3.4 Hz, 2H), 2.76 (m, J = 5.2 Hz, 8 H), 1.50 (app q, J = 3.8 Hz, 16H), 0.97 (t, J = 6.9 Hz, 12H); ³¹P NMR (162 MHz, CDCl₃) δ 33.0 (${}^{1}J_{PC}$ = 25.3 Hz, ${}^{2}J_{PC}$ = 7.5 Hz); ¹³C NMR (101 MHz, CDCl₃) δ 170.3, 134.8, 133.0, 130.5, 24.0 (${}^{1}J_{PC}$ = 15.3 Hz), 23.7 (${}^{1}J_{PC}$ = 4.7 Hz) 18.9 (${}^{1}J_{PC}$ = 47.6 Hz), 13.4 ppm. HRMS (ESI) m/z: measured 259.254033 C₁₆H₃₆P⁺ (M) requires 259.254914, HRMS (ESI) m/z: measured 165.010599 C₈H₅O₄ (M) requires 165.019332.

4.3.4. Tetrabutylphosphonium 2-carboxybenzenesulfonate (4). [15]

To a 10 mL round bottom flask equipped with a magnetic stir bar was added ⁿBu₄PBr (658 mg, 3 mmol), placed under an atmosphere of N2, and dissolved in CH2Cl2 (3 mL). Ammonium 2sulfobenzoic acid (1.02 g, 3 mmol) was added, followed by H₂O (1.5 mL), and the mixture stirred at rt for 15 h. The solution was diluted with H_2O (3 mL), extracted with CH_2Cl_2 (3 × 10 mL), and the combined organic extracts were washed with H2O (6 × 5 mL), dried (MgSO₄), filtered, and concentrated under reduced pressure. The residue was then dried in a vacuum oven at \sim 80 °C for 48 h to provide 0.942 g (68%) of **4** as a deep orange oil. Spectral data were consistent with literature values: ¹H NMR (400 MHz, CDCl₃) δ 14.63 (s, 1H), 8.06 (dd, I = 15.2, 7.3 Hz, 1H), 7.53 - 7.44 (m, 1H), 2.24 (q, J = 12.0, 8.6 Hz, 8H), 1.49 (dt, $I = 11.5, 7.0 \text{ Hz}, 16\text{H}), 1.05 - 0.81 \text{ (m, 12H)}; ^{13}\text{C NMR (100 MHz},$ CDCl₃) δ 168.1, 143.9, 132.9, 131.3, 130.3, 130.0, 127.1, 23.8 (d. I = 15.3 Hz), 23.6 (d, I = 4.7 Hz), 18.7 (d, I = 47.4 Hz), 13.4; ³¹P NMR (162 MHz, CDCl₃) δ 33.0; IR (neat): 2961, 1710, 1441, 1421, 1171, 1006, 910, 725 cm⁻¹; HRMS (ESI) m/z: measured 259.255262 $C_{16}H_{36}P^{+}$ (M) requires 259.254914, HRMS (ESI) m/z: measured 200.98760 C₇H₅O₅S (M) requires 200.986318.

4.3.5. Tetrabutylphosphonium 2-sulfonatobenzoate (5).

To a 25 mL round bottom flask equipped with a magnetic stir bar was added ⁿBu₄PBr (1.70 g, 5 mmol), placed under an atmosphere of N2, and diluted with CH2Cl2 (5 mL). Ammonium 2sulfobenzoic acid (1.10 g, 5 mmol) was added and the mixture was stirred at rt for 15 h then concentrated under reduced pressure. The resulting residue was reconstituted in acetone (10 mL), and the resulting suspension was filtered and rinsed with acetone $(3 \times 10 \text{ mL})$. The combined filtrates were concentrated under reduced pressure and the mixture was then treated with a solution of 1 M ⁿBu₄POH in MeOH (5 mL) and stirred at rt for 12 h. The resulting solution was concentrated under reduced pressure and reconstituted in acetone (10 mL) and the suspension was filtered through Celite and rinsed with acetone (3 \times 10 mL) and the filtrate was concentrated under reduced pressure. The ionic liquid was then dried further for an additional 48 h in a vacuum oven set to \sim 80 °C to provide 2.09 g (58% yield) of the title compound as a light orange oil. ¹H NMR (400 MHz, CDCl₃) δ 8.03 (dd, J = 8.0, 2.5 Hz, 1H), 7.40 (dd, I = 8.0, 4.4 Hz, 1H), 7.34 (d, I = 4.4 Hz, 1H), 7.29 (s, 1H), 2.39 - 2.33 (m, 16H), 1.52 - 1.49 (m, 32H), 0.98 0.94 (m, 24H); 13 C NMR (100 MHz, CDCl₃) δ 170.5, 144.4, 131.8, 129.5, 128.8, 128.2, 127.0, 52.6, 24.0 (d, J = 15.3 Hz), 23.8 (d, I = 4.8 Hz), 18.9 (d, I = 47.4 Hz), 13.5; ³¹P NMR (162 MHz, CDCl₃) δ 32.87; IR (neat): 1710, 1441, 1421, 1171, 1006, 910, 725 cm⁻1; HRMS (ESI) m/z: measured 259.255262 $C_{16}H_{36}P^{+}$ (M) requires 259.254914, HRMS (ESI) m/z: measured 200.987601 C₇H₅O₅S (M) requires 200.986318.

4.3.6. Tetrabutylphosphonium 3-hydroxybenzoate (6).[15]

To a 100 mL round bottom flask equipped with a magnetic stir bar under an atmosphere of N₂ was added ⁿBu₄PBr (2.00 g, 5.89 mmol) in MeOH (6 mL). To this solution was added 2 M KOH in MeOH (6.40 mmol, 3.2 mL). Precipitation was observed upon stirring at rt for 12 h, and the resulting suspension was filtered and rinsed with MeOH (3 \times 10 mL). To the filtrate was added 3-hydroxybenzoic acid (0.825 g, 5.98 mmol) and stirred at rt for 12 h. The resulting solution was concentrated under reduced pressure, reconstituted in acetone (10 mL), and filtered through Celite. The filter cake was washed with acetone (3 \times 10 mL) and the filtrate concentrated under reduced pressure. The residue was then dried in a vacuum oven at \sim 80 °C for 48 h to provide 2.28 g (97%) of 6 as a tan wax. Spectral data were consistent with literature values: ${}^{1}H$ NMR (400 MHz, CDCl₃) δ 8.21 (s, 1H), 7.52 (d, J = 7.5 Hz, 1H), 7.08 (t, J = 7.8 Hz, 1H), 6.82 (dd, J = 8.0, 1.6 Hz, 1H), 2.12 (m, I = 6.4 Hz, 8H), 1.93 (s, br, 1H), 1.42–1.26 (m, 16H), 0.85 (t, J = 6.8 Hz, 12H); ¹³C NMR (101 MHz, CDCl₃) δ 171.8, 158.1, 140.1, 128.2, 120.1, 117.6, 117.2, 23.8 (d, ${}^{1}J_{PC}$ = 11.8 Hz), 23.7, 18.6 (${}^{1}J_{PC}$ = 47.3 Hz), 13.5 ppm; ³¹P NMR (162 MHz, CDCl₃) δ 32.6 (${}^{1}J_{PC}$ = 25.3 Hz, ${}^{2}J_{PC}$ = 7.5 Hz); HRMS (ESI) m/z: measured 259.257274 $C_{16}H_{36}P^{+}$ (M) requires 259.254914, HRMS (ESI) m/z: measured 137.018566 C₇H₅O₃ (M) requires 137.024418.

4.3.7. Tetrabutylphosphonium 3-carboxybenzenesulfonate (7).

To a 25 mL round bottom flask equipped with a magnetic stir bar under an atmosphere of N2 was added "Bu4PBr (2.24 g, 10 mmol, 1 equiv.) and CH₂Cl₂ (10 mL). Then sodium 3sulfobenzoate (3.39 g, 10 mmol, 1 equiv.) was added, followed by H₂O (5 mL). The mixture was stirred vigorously at rt for 15 h. diluted with H₂O (10 mL) then extracted with CH₂Cl₂ $(3 \times 20 \text{ mL})$. The combined organic layers were washed with H₂O (6 × 10 mL), dried over MgSO₄, filtered and concentrated under reduced pressure. The ionic liquid was then dried further for an additional 48 h in a vacuum oven set to \sim 80 $^{\circ}$ C to provide 4.30 g (94%) of the title compound as a clear yellow oil. Spectral data were consistent with literature values: ¹H NMR (400 MHz, CDCl₃) δ 8.58 (s, 1H), 8.10 (d, J = 7.8 Hz, 1H), 8.01 (d, J = 7.7 Hz, 1H), 7.41 (t, J = 7.7 Hz, 1H), 7.18 (s, 1H), 2.34 – 2.20 (m, 8H), 1.55 -1.38 (m, 16H), 0.90 (t, J = 7.0 Hz, 12H); ¹³C NMR (100 MHz, CDCl₃) δ 167.6, 147.0, 130.6, 130.4, 130.3, 127.8, 127.5, 23.7 (d, J = 15.4 Hz), 23.4 (d, J = 4.7 Hz), 18.4 (d, J = 47.5 Hz), 13.3; ³¹P NMR (162 MHz, CDCl₃) δ 32.9; IR (neat): 3053, 1712, 1265, 1137, 1029, 907, 730 cm⁻¹; HRMS (ESI) *m/z*: measured 259.255297 $C_{16}H_{36}P^{+}$ (M) requires 259.254914, HRMS (ESI) m/z: measured 200.985369 C₇H₅O₅S (M) requires 200.986318.

4.3.8. Tetrabutylphosphonium 3-sulfonatobenzoate (8).

To a 25 mL round bottom flask equipped with a magnetic stir bar under an atmosphere of N₂ was added ⁿBu₄PBr (1.70 g, 5 mmol) in CH₂Cl₂ (5 mL). Then 2-sulfobenzoic acid ammonium salt (1.20 g, 5 mmol, 1 equiv.) was added and the mixture was stirred at rt for 15 h. The resulting solution was concentrated under reduced pressure and the residue was reconstituted in acetone (10 mL). The suspension was then filtered through Celite, rinsed with acetone $(3 \times 10 \text{ mL})$ and concentrated under reduced pressure. The crude mixture was then treated with a solution of 1 M ⁿBu₄POH in MeOH (1 M, 5 mL) and stirred at rt for 12 h. The resulting solution was concentrated under reduced pressure and reconstituted in acetone (10 mL) then the suspension was filtered through Celite, rinsed with acetone (3 × 10 mL) and concentrated under reduced pressure. The ionic liquid was then dried further for an additional 48 h in a vacuum oven set to \sim 80 °C to provide 2.16 g (60% yield) of the title compound as an orange oil. ¹H NMR (400 MHz, CDCl₃) δ 8.72 - 8.60 (m, 1H), 8.19 - 8.10 (m, 1H), 8.06 - 7.98 (m, 1H), 7.42 (q, J = 7.2 Hz, 1H), 2.40 - 2.21 (m, 16H), 1.66 - 1.34 (m, 32H), 1.02 -0.83 (m, 24H). 13 C NMR (100 MHz, CDCl₃) δ 195.0, 168.2, 155.3, 147.1, 130.61, 130.60, 128.1, 31.0, 23.9 (d, J = 17.3 Hz), 23.8 (d, J = 4.8 Hz), 18.8 (d, J = 47.3 Hz), 13.5; ³¹P NMR (162 MHz, CDCl₃) δ 32.96; IR (neat): 1712, 1265, 1137, 1029, 907, 730 cm⁻¹; HRMS (ESI) m/z: measured 259.255297 $C_{16}H_{36}P^{+}$ (M) requires 259.254914, HRMS (ESI) m/z: measured 200.985369 C₇H₅O₅S (M) requires 200.986318.

Declaration of Competing Interest

The authors declare that they have no known competing financial interests or personal relationships that could have appeared to influence the work reported in this paper.

Acknowledgements

The work in this manuscript was supported in part by the National Science Foundation CHE-1956170 and CBET-2031431 (BLA). The authors thank Dr. Evgenii Kovrigin for his assistance with conducting the NMR experiments.

Appendix A. Supplementary data

Supplementary data to this article can be found online at https://doi.org/10.1016/j.molliq.2022.119401.

References

- [1] P.K. Mohapatra, Dalton Trans. 46 (2017) 1730-1747.
- [2] N. Schaeffer, H. Passos, I. Billard, N. Papaiconomou, J.A.P. Coutinho, Critical Reviews in Environmental Science and Technology 48 (2018) 859-922.
- [3] S. P. M. Ventura, F. A. e Silva, M. V. Quental, D. Mondal, M. G. Freire, J. A. P. Coutinho, Chemical Reviews 2017, 117, 6984-7052.
- [4] Y. Zeng, J. Woods, S. Cui, Energy Convers. Manage. 244 (2021) 114520.
- [5] D. Zhao, P. Wang, Q. Zhao, N. Chen, X. Lu, Desalination 348 (2014) 26–32.
- [6] Y. Mok, D. Nakayama, M. Noh, S. Jang, T. Kim, Y. Lee, PCCP 15 (2013) 19510-
- [7] K. Takeshita, Cluj Napoca (Romania), Romania (2007).
 [8] D. Depuydt, L. Liu, C. Glorieux, W. Dehaen, K. Binnemans, Chem. Commun. 51 (2015) 14183-14186.
- [9] M. Abai, M.P. Atkins, A. Hassan, J.D. Holbrey, Y. Kuah, P. Nockemann, A.A. Oliferenko, N.V. Plechkova, S. Rafeen, A.A. Rahman, R. Ramli, S.M. Shariff, K.R. Seddon, G. Srinivasan, Y. Zou, Dalton Trans. 44 (2015) 8617-8624.
- [10] A.Z. Haddad, A.K. Menon, H. Kang, J.J. Urban, R.S. Prasher, R. Kostecki, Environ. Sci. Technol. 55 (2021) 3260-3269.
- [11] Y. Cai, W. Shen, J. Wei, T.H. Chong, R. Wang, W.B. Krantz, A.G. Fane, X. Hu, Environ. Sci. Water Res. Technol. 1 (2015) 341-347.
- [12] R. Semiat, Environ. Sci. Technol. 42 (2008) 8193-8201.
- [13] K. Fukumoto, H. Ohno, Angew. Chem. Int. Ed. 46 (2007) 1852–1855.
- [14] Y. Kohno, H. Ohno, PCCP 14 (2012) 5063-5070.
- [15] T. Ando, Y. Kohno, N. Nakamura, H. Ohno, Chem. Commun. 49 (2013) 10248-10250.
- Y. Fukaya, H. Ohno, PCCP 15 (2013) 4066-4072.
- Y. Kohno, H. Arai, S. Saita, H. Ohno, Aust. J. Chem. 64 (2011) 1560-1567.
- [18] M.B. Hillyer, B.C. Gibb, Annu. Rev. Phys. Chem. 67 (2016) 307–329.
- [19] J.G. Davis, K.P. Gierszal, P. Wang, D. Ben-Amotz, Nature 491 (2012) 582-585.
- [20] H. Kang, D.E. Suich, J.F. Davies, A.D. Wilson, J.J. Urban, R. Kostecki, Communications Chemistry 2 (2019) 51.
- S. S, S. Gunasekaran, S. S, Spectrochimica Acta. Part A, Molecular and Biomolecular Spectroscopy 2014, 132C, 130-141.
- N.V. Karimova, M. Luo, V.H. Grassian, R.B. Gerber, PCCP 22 (2020) 5046-5056.
- [23] J.A. Amador-Balderas, M.-A. Martínez-Sánchez, R.E. Ramírez, F. Méndez, F.J. Meléndez, Molecules 25 (2020) 1631.
- [24] S. Böhm, P. Fiedler, O. Exner, New J. Chem. 28 (2004) 67-74.
- E. Mullins, R. Oldland, Y.A. Liu, S. Wang, S.I. Sandler, C.-C. Chen, M. Zwolak, K.C. Seavey, Ind. Eng. Chem. Res. 45 (2006) 4389-4415.
- [26] T. Mu, J. Rarey, J. Gmehling, Ind. Eng. Chem. Res. 46 (2007) 6612-6629.

- [27] T. Lemaoui, A.S. Darwish, N.E.H. Hammoudi, F. Abu Hatab, A. Attoui, I.M. Alnashef, Y. Benguerba, Ind. Eng. Chem. Res. 59 (2020) 13343-13354.
- [28] H. Kang, D.E. Suich, J.F. Davies, A.D. Wilson, J.J. Urban, R. Kostecki, Communications Chemistry (2019) 2.
- [29] U. Adhikari, S. Scheiner, Chem. Phys. 440 (2014) 53–63.
- [30] J.G. Davis, S.R. Zukowski, B.M. Rankin, D. Ben-Amotz, J. Phys. Chem. B 119 (2015) 9417–9422.
- [31] N.N. Nasief, D. Hangauer, J. Med. Chem. 57 (2014) 2315-2333.
- [32] M. Zanatta, V.U. Antunes, C.F. Tormena, J. Dupont, F.P. Dos Santos, PCCP 21 (2019) 2567-2571.
- [33] G. Pages, V. Gilard, R. Martino, M. Malet-Martino, Analyst 142 (2017) 3771-3796.
- [34] X. Wang, Y. Chi, T. Mu, J. Mol. Liq. 193 (2014) 262–266.
 [35] S. N. S. Sharon I. Lall-Ramnarine, Eddie D. Fernandez, Chanele Rodriguez, Sujun Wei, Mallory Gobet, J. R. P. Jayakody, Surajdevprakash B. Dhiman, James F. Wishart, Journal of the Electrochemical Society 2017, 164, H5150-H5159.
- [36] R. Scheu, Y. Chen, H.B. de Aguiar, B.M. Rankin, D. Ben-Amotz, S. Roke, J. Am. Chem. Soc. 136 (2014) 2040-2047.
- [37] R. Scheu, B.M. Rankin, Y. Chen, K.C. Jena, D. Ben-Amotz, S. Roke, Angew. Chem. Int. Ed. 53 (2014) 9560-9563.
- [38] A. Mix, P. Jutzi, B. Rummel, K. Hagedorn, Organometallics 29 (2010) 442–447.
 [39] J. Guest, P. Kiraly, M. Nilsson, G. Morris, J. Magn. Reson. 2 (2021) 733–739.
- [40] W.C. Still, M. Kahn, A. Mitra, J. Organic Chemistry 43 (1978) 2923–2925.